Modeling of Multilayered Media Green's Functions With Rough Interfaces

François Jonard, Frédéric André, Nicolas Pinel, Craig Warren, Harry Vereecken, and Sébastien Lambot

***Abstract*—Horizontally stratified media are commonly used to represent naturally occurring and manmade structures, such as soils, roads, and pavements, when probed by ground-penetrating radar (GPR). Electromagnetic (EM) wave scattering from such multilayered media is dependent on the roughness of the interfaces. In this study, we developed a closed-form asymptotic EM model taking into account random rough layers based on the scalar Kirchhoff-tangent plane approximation (SKA) model, which we combined with planar multilayered media Green's functions. In order to validate our extended SKA model, we conducted simulations using a numerical EM solver based on the finite-difference time-domain (FDTD) method. We modeled a medium with three layers – a base layer of perfect electric conductor (PEC), overlaid by two layers of different materials with rough interfaces. The reflections at the first and at the second interface were both well reproduced by the SKA model for each roughness condition. For the reflection at the PEC surface, the extended SKA model slightly overestimated the reflection, and this overestimation increased with the roughness amplitude. A good agreement was also obtained between the FDTD simulation input values and inverted root mean square (RMS) height estimates of the top interface, while the inverted RMS heights of the second interface were slightly overestimated. The accuracy and the performances of our asymptotic forward model demonstrate promising perspectives for simulating rough multilayered media, and hence, for the full waveform inversion of GPR data to non-invasively characterize soils and materials.**

***Index Terms*—FDTD, gprMax, Green's function, ground-penetrating radar (GPR), Kirchhoff-tangent plane approximation, model inversion, multilayered media, radar, rough interfaces, scattering**

I. Introduction

Ground-penetrating radar (GPR) is a widely used geophysical method for non-destructive probing of media in many different fields such as agricultural and environmental engineering, civil engineering, hydrology, and archaeology [1], [2]. It allows rapid data collection and has been successfully used to characterize a range of different media (e.g., soils, pavements, trees) [3]–[6] or to detect embedded objects [7], [8].

Scattering by random rough interfaces of stratified media such as soils and roadways has to be accounted for to accurately retrieve the electromagnetic (EM) properties of the different layers by GPR. When the roughness amplitude becomes non negligible compared to the radar wavelength, specular reflections are decreased and diffuse reflections occur at the rough interfaces, leading to smaller echoes in the recorded GPR data.

A wide range of asymptotic EM models have been proposed to describe scattering from random rough interfaces. These models have mainly been developed for one-layer media with a unique rough interface ([9] and references therein, [10]–[12]). Some of these models have been extended in order to account for the roughness of both interfaces of this single layer configuration. Amongst others, the small perturbation method (SPM) has been extended to account for two interfaces [13]–[16] and is valid for small height variations compared to the EM wavelength. Soubret *et al.* [17] extended the reduced Rayleigh equations to the case of two slightly rough interfaces. Fuks *et al.* [18]–[20] developed a model for scattering from a slightly rough surface overlying a strongly rough surface compared to the incident EM wavelength. Pinel *et al.* [21], [22] extended the Kirchhoff-tangent plane approximation (KA) reduced to the geometric optics approximation to two random rough interfaces. Also, reductions of the KA to the scalar KA (SKA) have been proposed for dealing with the coherent scattering from random rough layers [23]–[25]. Concerning the so-called unified models for random rough layers, we can cite the full-wave model [26], [27], the small slope approximation method (SSA) [28], as well as the radiative transfer model [29].

In contrast to single rough layer EM models, literature on EM models for multilayered media with multiple rough interfaces remains sparse [30], and only a few models dealing with more than two rough interfaces have been developed. To the best of our knowledge, only classical asymptotic models exist, and are only valid for slightly rough interfaces [31]–[40]. The proposed solutions are generally based on the SPM. One exception is the recent paper by Afifi *et al.* [38], where both the SPM and the SSA have been applied and investigated. The advantage of using the SSA is the extension of the validity domain to rougher surfaces. Considering the backscattering from rough interfaces at normal incidence, i.e., incidence angle classically used for an off-ground GPR configuration, this

This research was supported in part by the German Research Foundation (DFG) under Grant JO 1262/2-1, in part by the Fonds de la Recherche Scientifique (FRS-FNRS, Belgium), and in part by the European Cooperation in Science and Technology (COST) Action TU1208 "Civil Engineering Applications of Ground Penetrating Radar". Computational resources have been provided by the Consortium des équipements de Calcul Intensif (CÉCI), funded by the FRS-FNRS under Grant No. 2.5020.11.

F. Jonard, H. Vereecken, Agrosphere (IBG-3), Institute of Bio- and Geosciences, Forschungszentrum Juelich GmbH, 52425 Juelich, Germany. (e-mail: f.jonard@fz-juelich.de, h.vereecken@fz-juelich.de).

F. Jonard, F. André, S. Lambot, Earth and Life Institute, Université catholique de Louvain, 2 Croix du Sud, Box L7.05.02, 1348 Louvain-la-Neuve, Belgium. (e-mail: francois.jonard@uclouvain.be, frederic.andre@uclouvain.be, sebastien.lambot@uclouvain.be).

N. Pinel, Icam school of Engineering, 35 Avenue du Champ de Manoeuvres, 44470 Carquefou, France. (e-mail: nicolas.pinel@icam.fr).

C. Warren, Department of Mechanical and Construction Engineering, Northumbria University, Newcastle upon Tyne, NE1 8ST, United Kingdom. (e-mail: craig.warren@northumbria.ac.uk).

implies that the coherent component is the main contributor to the total scattering process. However, if only the first-order of the SPM is used, the coherent scattered intensity reduces to that of flat surfaces. Therefore, it is necessary to use at least the second-order SPM [40] or the SSA [38]. For the SSA, the solution proposed in [38] is restricted to Gaussian height distributions and correlation functions. Regarding the SPM, an expression of the second-order coherent normalized radar cross section (NRCS) has been derived recently [40], but only for two-dimensional problems.

In this study, we present a new closed-form asymptotic EM model taking into account random rough layers based on the scalar Kirchhoff-tangent plane approximation (SKA) model that we combined with planar multilayered media Green's functions and a full-wave, closed-form radar-antenna model. This generalizes the model of Jonard *et al.* [41], in which only scattering in reflection from the rough surface, i.e., the upper air/soil medium interface, was taken into account. The new developed model applies to multilayered media with random rough layers and it takes into account the scattering in transmission through the rough interfaces. The objective is also to propose an easily implementable and computationally efficient model suitable for inversion, using a three-dimensional (3-D) analytical formulation. This new model was validated through comparisons with a 3-D reference GPR simulation software, namely, gprMax [42], and the performance of the model for retrieving medium properties from GPR full-wave inversion [43] was investigated.

The paper begins with a description of the modeling of the planar multilayered media Green's functions in Section II. Section III provides a description of the proposed EM model accounting for the scattering from multilayered media with random rough interfaces. Section IV then presents the finite-difference time-domain (FDTD) simulations carried out using gprMax and Section V introduces the inversion of the proposed model. In Section VI we present and discuss the main results, and lastly, we give a summary and concluding remarks in Section VII.

II. Planar multilayered media Green's functions

Electromagnetic wave propagation in 3-D planar layered media can be described using closed-form Green's functions in the frequency domain, which are exact solutions of Maxwell's equations [43], [44]. For the particular case of radar applications, the Green's functions usually represent the backscattered electric field for a unit strength electric source. The Green's function is first calculated in the spectral domain and, subsequently, transformed into the 3-D spatial domain through a Sommerfeld's integral [45]. The spectral domain Green's function is calculated using the global reflection coefficients of the multilayered medium obtained using a recursive scheme [44].

III. Interface roughness model

In general, random rough surfaces are assumed to be stationary with a Gaussian height distribution. A rough surface can therefore be described by the following statistical quantities: the root mean square (RMS) of the surface heights, and the spatial autocorrelation function, with its associated spatial autocorrelation length [46]. The shape of the autocorrelation function is usually taken as either Gaussian or exponential, depending on the considered rough surfaces.

A. Single interface

To account for the impact of the roughness of a single surface on radar EM wave propagation and scattering in the specular direction, the Ament model [47], [48] is usually used. This model, which is derived from the Kirchhoff-tangent plane scattering theory, describes the scattering losses in the specular direction due to the reflection onto a random rough interface. This model has been applied in several studies investigating the roughness effect on EM wave scattering over sea or soil surfaces [41], [49] and for rough building materials [50]. In this model, the global surface reflection coefficient is multiplied by a scattering loss factor ($\mathcal{A}$), which is based on the Rayleigh parameter as a function of frequency, given by (1).

$$\mathcal{A} = e^{-g/2} \tag{1}$$

where

$$g = \left(\frac{4\pi s_r \cos\theta_i}{\lambda} \right)^2 \tag{2}$$

with θ_i the incidence angle, s_r the RMS of the surface heights, and λ the wavelength in free space. The modified reflection coefficient r^m that models the reduction of the reflection amplitude in the specular direction is then defined by:

$$r^m_{TE} = \mathcal{A} \ r_{TE} \tag{3}$$

$$r^m_{TM} = \mathcal{A} \ r_{TM} \tag{4}$$

where r_{TE} and r_{TM} are the transverse electric- (TE) and transverse magnetic- (TM) mode Fresnel reflection coefficients for a perfectly flat surface, respectively. Equations (3) and (4) assume that the surface heights have a Gaussian distribution with large surface curvatures compared to the electromagnetic wavelength, as well as negligible shadowing and multiple scattering effects [48]. In the present study, normal incidence is considered ($\theta_i = 0$), so the shadowing and multiple scattering effects can be neglected.

B. Extension to a multilayered system

For the case of a multilayered system, as shown in Figure 1 (N layers, $N-1$ interfaces), the problem becomes more complex, as multiple transmissions and reflections occur inside the multilayered medium.

Recently, the SKA has been extended to the case of a single layer problem with two interfaces [21]. We present here the equations for a reflection inside a layer Ω_n onto a layer Ω_{n+1} with thickness d_{n+1}. In this case, the classical expression of the so-called equivalent Fresnel reflection coefficient R_n for the flat case is given by (5).

$$R_n = r_n + \frac{(1-r_n^2) r_{n+1} e^{-2\Gamma_{n+1} d_{n+1}}}{1 + r_n r_{n+1} e^{-2\Gamma_{n+1} d_{n+1}}}, \tag{5}$$

with r_n and r_{n+1}, the Fresnel reflection coefficients onto the upper and lower interfaces of the considered layer, respectively, and Γ_{n+1}, the vertical component of the propagation wavenumber of the wave inside the layer Ω_{n+1} multiplied by *j*.

Equation (5) can be further simplified as:

$$R_n = \frac{r_n + r_{n+1} e^{-2\Gamma_{n+1} d_{n+1}}}{1 + r_n r_{n+1} e^{-2\Gamma_{n+1} d_{n+1}}}, \tag{6}$$

By contrast, for the general case of independent random rough interfaces, the expression can be written as in [24], [25]:

$$R_{n,rough} = r_n \mathcal{A}_n + \frac{(1 - r_n^2) r_{n+1} e^{-2\Gamma_{n+1} d_{n+1}} \mathcal{A}_{n+1}}{1 + r_n r_{n+1} e^{-2\Gamma_{n+1} d_{n+1}} \mathcal{A}_{r(n+1,n)} \mathcal{A}_{r(n+1,n+2)}}, \tag{7}$$

The attenuation terms related to the roughness can be formulated as follows for Gaussian statistics (i.e., Gaussian height probability density function):

$$\mathcal{A}_n = e^{-2[-j\,\Gamma(n)\,s_r(n)]^2} \tag{8}$$

$$\mathcal{A}_{n+1} = e^{-2[-j\,\Gamma(n+1)\,s_r(n+1)]^2 - s_r(n)^2[-j\,\Gamma(n) + j\,\Gamma(n+1)]^2} \tag{9}$$

$$\mathcal{A}_{r(n+1,n)} = e^{-2[-j\,\Gamma(n+1)\,s_r(n)]^2} \tag{10}$$

$$\mathcal{A}_{r(n+1,n+2)} = e^{-2[-j\,\Gamma(n+1)\,s_r(n+1)]^2} \tag{11}$$

in which $s_r(n)$ is the RMS of the surface heights of the interface Σ_n separating layers Ω_n, and Ω_{n+1}.

With a view to extending the formulation by iterations to multilayers, expression (7) should be rewritten by introducing $r_{n+1,rough}$. It corresponds to the Fresnel reflection coefficient in the TE or TM polarization modified by the roughness of the considered interface, as expressed in Equations (3) or (4), respectively. For interface $n+1$, it mathematically corresponds to

$$r_{n+1,rough} = r_{n+1}\, e^{-2[-j\,\Gamma(n+1)\,s_r(n+1)]^2}, \tag{12}$$

so that Equation (7) can be rewritten as

$$R_{n,rough} = r_n \mathcal{A}_n + \frac{(1 - r_n^2) r_{n+1,rough} e^{-2\Gamma_{n+1} d_{n+1}} \mathcal{A}_{t(n,n+1)}}{1 + r_n r_{n+1,rough} e^{-2\Gamma_{n+1} d_{n+1}} \mathcal{A}_{r(n+1,n)}}, \tag{13}$$

with

$$\mathcal{A}_{t(n,n+1)} = e^{-s_r(n)^2[-j\,\Gamma(n) + j\,\Gamma(n+1)]^2} \tag{14}$$

the last term $A_{t(n,n+1)}$ corresponding physically to the decrease of the amplitude of the wave during its transmission between layer Ω_n and layer Ω_{n+1}, due to the roughness of interface Σ_n.

The extension of the approach for a single layer with two interfaces to a multilayered system can be performed as explained below. First, for the flat case, it can be shown that the equivalent Fresnel reflection coefficient R_n has the same formal expression as for a single layer (2 interfaces) in Equation (5), except that the Fresnel reflection coefficient r_{n+1} must be replaced by the equivalent Fresnel reflection coefficient R_{n+1}. Then, the resolution of this system can be made in several ways. Here, following [43], it is resolved within the calculation of the Green's function by using a recursive scheme and by starting with the lower interface (Σ_{N-1}). For the rough case, the same method is used, and the modification from $r_{n+1,rough}$ to $R_{n+1,rough}$ must also be made:

$$R_{n,rough} = r_n \mathcal{A}_n + \frac{(1 - r_n^2) R_{n+1,rough} e^{-2\Gamma_{n+1} d_{n+1}} \mathcal{A}_{t(n,n+1)}}{1 + r_n R_{n+1,rough} e^{-2\Gamma_{n+1} d_{n+1}} \mathcal{A}_{r(n+1,n)}}, \tag{15}$$

for all $n \leq N-2$; at the initialization $n = N-1$ (corresponding to the lower interface Σ_{N-1}), we have

$$\begin{aligned} R_{N-1,rough} &= r_{N-1,rough} \\ &= r_{N-1}\, e^{-2[-j\,\Gamma(N-1)\,s_r(N-1)]^2} \end{aligned} \tag{16}$$

IV. Numerical simulation using a FDTD model

In order to validate the extended SKA model we conducted a series of numerical simulations. We used gprMax [42], which is an open source software that simulates EM wave propagation in the time domain. gprMax uses Yee's algorithm [51] to solve Maxwell's equations in 3-D using the finite-difference time-domain (FDTD) method. In this paper, comparisons between our frequency domain model and gprMax were performed using fast Fourier transforms.

We used a spatial resolution of $\Delta x = \Delta y = \Delta z = 0.0025$ m, and a temporal resolution of $\Delta t = 4.81 \times 10^{-12}$ s (to satisfy the Courant-Friedrichs-Lewy condition). The domain size was $2.5 \times 2.5 \times 1.05$ m, which was enabled through the use of efficiently performing perfectly matched layer (PML) absorbing boundary conditions [52]. A higher-order split-field PML was introduced by Correia and Jin in 2005 [53], and since then a series of different unsplit implementations have been reported [54]–[56], including a multipole PML method [57]. A Hertzian dipole was used as a point source, polarised in the x-direction, and excited with a waveform having the shape of the first derivative of a Gaussian. The centre frequency of this waveform was 900 MHz and the main range was 200 MHz – 2000 MHz. The source and the receiver (which stored the time histories of the electric and magnetic field components) were collocated in the centre of the $x-y$ plane, and at a height of $z = 0.85$ m from the base of the model. The geometrical model used for these FDTD simulations, shown in Figure 2, consisted of two material layers: the upper material layer had a relative permittivity of 4 ($\epsilon_r = 4$) and an average thickness of 30 cm, and the lower layer had a relative permittivity of 10 ($\epsilon_r = 10$) and an average thickness of 20 cm. We used an electrical conductivity of zero for the two layers in order to maximize scattering from the interfaces, and hence, to better compare both modeling approaches. Our medium is therefore non dispersive. A perfect electric conductor (PEC) layer was located at the base of the model in order to receive echoes that were transmitted through the second interface. Two interfaces

were considered as potentially rough: the upper interface of the top material layer, and the interface between the two material layers. Six different RMS values of the surface heights were considered for both of them (i.e., $s_r = \{0; 0.005; 0.01; 0.015; 0.02; 0.025\}$ m), leading to 36 combinations of roughness conditions. A Gaussian spatial autocorrelation function with a spatial autocorrelation length of 0.15 m was used. This value was selected as a compromise between having a large enough autocorrelation length so that the surface has gentle surface slopes to remain in the validity domain of the extended SKA model (typically, RMS slopes less than about 0.3), as the multiple reflections from the same interface and shadowing are not accounted for, and by keeping a problem of limited size to be efficiently computable. For each roughness condition, 50 Monte-Carlo realizations were performed in order to emulate infinitely large surfaces.

A. Green's functions from the FDTD models

The electric field calculated in gprMax ($b(t)$) includes the direct transmission between the transmitter and receiver (R_i), as well as the convolution with the source signal ($a(t)$), t being the propagation time. In order to calculate the layered media Green's functions, which consider a unit source for each frequency, from gprMax and compare them to those provided by the proposed model, these two contributions need to be filtered out. As for real radar systems, the radar equation of Lambot *et al.* [43], [58] can be applied to FDTD simulated data. In the frequency domain, this equation is formulated as:

$$S_{11}(\omega) = \frac{B(\omega)}{A(\omega)} = R_{\mathrm{i}}(\omega) + \frac{T(\omega)\, G^{\uparrow}_{\mathrm{xx}}(\omega)}{1 - R_{\mathrm{s}}(\omega)\, G^{\uparrow}_{\mathrm{xx}}(\omega)} \tag{17}$$

where $S_{11}(\omega)$ is the ratio between the received electric field $B(\omega)$ and the electric source $A(\omega)$, ω being the angular frequency; $R_{\mathrm{i}}(\omega)$ is the direct transmission between the transmitter and receiver (free-space response); $T(\omega) = T_{\mathrm{i}}(\omega)T_{\mathrm{s}}(\omega)$ where $T_{\mathrm{i}}(\omega)$ is the antenna global transmission coefficient for incident fields and $T_{\mathrm{s}}(\omega)$ is the antenna global transmission coefficient for scattered fields; $R_{\mathrm{s}}(\omega)$ is the antenna global reflection coefficient for scattered fields; and $G^{\uparrow}_{\mathrm{xx}}(\omega)$ is the planar layered medium Green's function.

For the FDTD simulations, Equation (17) can be rewritten as:

$$B(\omega) = A(\omega)R_{\mathrm{i}}(\omega) + A(\omega)\frac{T(\omega)\, G^{\uparrow}_{\mathrm{xx}}(\omega)}{1 - R_{\mathrm{s}}(\omega)\, G^{\uparrow}_{\mathrm{xx}}(\omega)} \tag{18}$$

Defining $H_{\mathrm{i}} = A(\omega)R_{\mathrm{i}}(\omega)$ and $H = A(\omega)T(\omega)$, then Equation (18) becomes:

$$B(\omega) = H_{\mathrm{i}}(\omega) + \frac{H(\omega)\, G^{\uparrow}_{\mathrm{xx}}(\omega)}{1 - R_{\mathrm{s}}(\omega)\, G^{\uparrow}_{\mathrm{xx}}(\omega)} \tag{19}$$

As the receiver reduces to a field point in the FDTD simulations (i.e., there is no physical antenna in the models), $R_{\mathrm{s}}(\omega) = 0$ and Equation (19) becomes:

$$B(\omega) = H_{\mathrm{i}}(\omega) + H(\omega)\, G^{\uparrow}_{\mathrm{xx}}(\omega) \tag{20}$$

which links the electric field calculated in the FDTD simulations to the Green's function defined above.

The virtual gprMax antenna functions H_{i} and H may be determined by solving a system of two equations for the two unknowns H_{i} and H. H_{i} is directly obtained from a FDTD simulation with free-space conditions in which $G^{\uparrow}_{\mathrm{xx}}(\omega) = 0$. Once H_{i} is known, H can be calculated by solving Equation (19) for a known configuration (e.g., the source and receiver at some distance over an infinite PEC) for which $B(\omega)$ can be obtained from the FDTD simulation, and $G^{\uparrow}_{\mathrm{xx}}(\omega)$ can be analytically calculated.

V. Inversion

The inverse problem consisted of finding the minimum of the following objective function:

$$\phi(\mathbf{p}) = \left|\mathbf{G}^{\uparrow *}_{\mathrm{xx}}(\omega) - \mathbf{G}^{\uparrow}_{\mathrm{xx}}(\mathbf{p},\omega)\right|^{\mathrm{T}} \left|\mathbf{G}^{\uparrow *}_{\mathrm{xx}}(\omega) - \mathbf{G}^{\uparrow}_{\mathrm{xx}}(\mathbf{p},\omega)\right| \tag{21}$$

where $\mathbf{G}^{\uparrow *}_{\mathrm{xx}}$ is the Green's function obtained from the FDTD simulations, $\mathbf{G}^{\uparrow}_{\mathrm{xx}}$ is the Green's function simulated with the extended SKA model, and $\mathbf{p}$ is the parameter vector to be estimated and is defined as $\mathbf{p} = [s_{r1}, s_{r2}]$. Optimization was performed using the multi-level coordinate search (MCS) algorithm [59].

VI. Results and Discussion

A. Green's functions comparisons

Figure 3 shows the Green's functions computed using the asymptotic extended SKA model and using FDTD simulations (mean of 50 Monte Carlo simulations) in the frequency ($\mathbf{G}^{\uparrow}_{\mathrm{xx}}(\omega)$) and time ($\mathbf{g}^{\uparrow}_{\mathrm{xx}}(t)$) domains for the configuration with perfectly flat interfaces. Both models naturally agree perfectly. Figures 4 and 5 show the Green's functions computed using the asymptotic extended SKA model and using FDTD simulations (mean of 50 Monte Carlo simulations) in the frequency ($\mathbf{G}^{\uparrow}_{\mathrm{xx}}(\omega)$) and time ($\mathbf{g}^{\uparrow}_{\mathrm{xx}}(t)$) domains, for different interface roughness conditions. In the time domain, the reflection at the first interface is always very well reproduced by the extended SKA model for each roughness condition. The reflection at the second interface is also well reproduced. For the reflection at the PEC surface, the extended SKA model slightly overestimates the reflection, and this overestimation increases with the roughness amplitude. The overestimation also increases more significantly with an increase of the roughness amplitude at the second interface compared to an equivalent increase of the roughness amplitude at the first interface. In the frequency domain, the amplitude of the Green's function is also well reproduced by the extended SKA model for different roughness conditions on the first interface when the second interface is considered as flat. When applying roughness to the second interface, the extended SKA model slightly overestimates the amplitude of the Green's function. This overestimation increases both with increasing frequency and with increasing roughness amplitude. Finally, the Green's function phase in the frequency domain, and thereby the propagation time in the time domain, are systematically well described by the model, though some discrepancies with the FDTD simulation data appear as roughness increases.

B. Analysis of the objective function

Figure 6 shows the sections of the logarithm of the objective function (OF) (21) for five parameters, i.e., the RMS of the surface heights of the first (s_{r1}) and second (s_{r2}) interfaces, the thickness of the first layer (d_1), and the relative dielectric permittivity of the first (ϵ_{r1}) and second (ϵ_{r2}) layers in six parameter planes $s_{r1} - s_{r2}$, $d_1 - s_{r1}$, $\epsilon_{r1} - s_{r1}$, $\epsilon_{r1} - s_{r2}$, $\epsilon_{r2} - s_{r1}$, and $\epsilon_{r2} - s_{r2}$. The OF values were calculated using the FDTD simulation data (mean of 50 Monte-Carlo simulations) obtained for RMS height values of 0.015 m at both interfaces, and by considering a relatively large parameter space ($0 < s_{ri} < 0.03$ m, $1 < \epsilon_{r1/2} < 15$ and $0.1 < d_1 < 0.4$ m), which contained the exact solutions. The range of each parameter was divided into 200 discrete values resulting in 40 000 OF values for each section. In Figure 6(a), the minimum of the OF is unique. The two roughness parameters do not appear to be significantly correlated, which is expected as the two layers are well separated in the time domain. In Figures 6(b-f), local minima can be observed, while the global minimum always remains unique. The sensitivity of the roughness parameters is significantly smaller than that of the layer thickness and relative dielectric permittivity parameters. The reduced sensitivity with respect to the roughness parameters may lead to significant errors in their reconstruction, especially for real data which are inherently subject to errors that are expected to flatten the topography of the objective function. The minimum of the OF corresponds well to the true values for the layer thickness and relative dielectric permittivity parameters, while it does not correspond exactly to the true parameter values for the roughness parameters, especially for s_{r2}. The errors in the estimation of s_{r2} are due to differences between the extended SKA model and the FDTD simulation data, as noticed previously in Figures 4 and 5.

C. Roughness parameters inversion

Figure 7 depicts the inverted RMS of the surface heights of the two interfaces (s_{r1} and s_{r2}) compared to the RMS values used as input for the 50 FDTD Monte-Carlo simulations. A good agreement was obtained between the FDTD simulation input values and the inverted s_{r1} estimates, except for the specific case of a flat top interface ($s_{r1} = 0$) and a rough lower interface ($s_{r2} > 0$). Inverted s_{r2} data slightly overestimate the FDTD simulation input values and the overestimation continuously increases with increasing s_{r2}. These results demonstrate the consistency of the extended SKA model. Nevertheless, we observe increasing errors for s_{r2} as roughness increases. This is to be attributed to the overestimation by the asymptotic model of the amplitude of the third reflection (see Figures 4(a, c, and e) and 5). Hence, the asymptotic model underestimates the scattering and, therefore, inverted roughness values of the second interface are overestimated to compensate for this underestimation.

VII. Summary and Conclusion

A closed-form asymptotic EM model taking into account random rough layers was combined with planar multilayered media Green's functions in order to invert radar signals for non-invasive quantification of medium properties. The validation of this extended SKA model was performed using a numerical approach based on the FDTD method. The FDTD simulations were carried out using gprMax software to model EM wave propagation in a multilayered medium composed of two layers above a PEC. Two interfaces, i.e, the surface of the top layer and the interface between the two layers, were considered as rough with RMS of the surface heights ranging from 0 to 0.025 m. The validation was performed by comparing the Green's functions derived from the asymptotic model and the ones derived from the numerical simulations. In order to calculate the layered media Green's functions from the FDTD simulations, the direct transmission between the transmitter and receiver as well as the source signal were filtered out from the electric field values obtained by gprMax.

The results show that, in the time domain, the reflection at the first interface is always very well reproduced by the extended SKA model for each roughness condition, as well as the reflection at the second interface. In contrast, the extended SKA model slightly overestimates the reflection at the PEC surface and this overestimation increases with the roughness amplitude. In the frequency domain, the amplitude of the Green's function is also well reproduced by the extended SKA model for different roughness conditions on the first interface and when considering the second interface as flat. For roughness conditions at the second interface, the extended SKA model slightly overestimates the amplitude of the Green's function, and this overestimation increases with increasing frequency and with increasing roughness amplitude. A good agreement is also obtained between the FDTD simulation input values and the inverted RMS height values of the top interface, while the inverted RMS height values of the second interface are slightly overestimated. This is to be attributed to the overestimation by the asymptotic model of the amplitude of the reflection on the PEC, due to an underestimation of the scattering at the second interface. It has to be noted that the proposed model has been validated for roughness amplitudes (RMS heights) up to $\lambda/4$ and surface slopes (RMS slopes) up to 0.24, λ being the smallest wavelength associated with the highest frequency $f = 1.5$ GHz considered in this study and the relative dielectric permittivity $\epsilon_r = 4$ of the layer above the second (inner) rough interface. These results demonstrate the consistency of the extended SKA model and the promising perspectives for rough multilayered media reconstruction using full-wave inversion of radar data.

Acknowledgments

We are grateful to the editorial board and the anonymous reviewers for their constructive comments and suggestions that helped to improve the previous version of this paper.

References

[1] E. Slob, M. Sato, and G. Olhoeft, "Surface and borehole ground-penetrating-radar developments," *Geophysics*, vol. 75, no. 5, pp. A103–A120, 2010.

[2] A. Klotzsche, F. Jonard, M. C. Looms, J. van der Kruk, and J. A. Huisman, "Measuring soil water content with ground penetrating radar: a decade of progress," *Vadose Zone Journal*, vol. 17, p. 180052, 2018.

[3] J. Minet, A. Wahyudi, P. Bogaert, M. Vanclooster, and S. Lambot, "Mapping shallow soil moisture profiles at the field scale using full-waveform inversion of ground penetrating radar data," *Geoderma*, vol. 161, no. 3-4, pp. 225–237, 2011.

[4] F. Jonard, L. Weihermüller, K. Z. Jadoon, M. Schwank, H. Vereecken, and S. Lambot, "Mapping field-scale soil moisture with L-band radiometer and ground-penetrating radar over bare soil," *IEEE Transactions on Geoscience and Remote Sensing*, vol. 49, no. 8, pp. 2863–2875, 2011.

[5] F. André, F. Jonard, M. Jonard, and S. Lambot, "In situ characterization of forest litter using ground-penetrating radar," *Journal of Geophysical Research: Biogeosciences*, vol. 121, no. 3, pp. 879–894, 2016.

[6] S. Zhao and I. L. Al-Qadi, "Development of an analytic approach utilizing the extended common midpoint method to estimate asphalt pavement thickness with 3-d ground-penetrating radar," *NDT and E International*, vol. 78, pp. 29–36, 2016.

[7] V. Pérez Gracia, J. A. Canas, L. G. Pujades, J. Clapés, O. Caselles, F. Garcia, and R. Osorio, "Gpr survey to confirm the location of ancient structures under the valencian cathedral (spain)," *Journal of Applied Geophysics*, vol. 43, no. 2, pp. 167–174, 2000.

[8] C. W. Chang, C. H. Lin, and H. S. Lien, "Measurement radius of reinforcing steel bar in concrete using digital image gpr," *Construction and Building Materials*, vol. 23, no. 2, pp. 1057–1063, 2009.

[9] Y. S. Kaganovskii, V. D. Freilikher, E. Kanzieper, Y. Nafcha, M. Rosenbluh, and I. M. Fuks, "Light scattering from slightly rough dielectric films," *Journal of the Optical Society of America A*, vol. 16, no. 2, pp. 331–8, 1999.

[10] A. G. Yarovoy, C. N. Vazouras, J. G. Fikioris, and L. P. Ligthart, "Numerical simulations of the scattered field near a statistically rough air-ground interface," *IEEE Transactions on Antennas and Propagation*, vol. 52, pp. 780–789, 2004.

[11] B. Sai and L. P. Ligthart, "GPR phase-based techniques for profiling rough surfaces and detecting small, low-contrast landmines under flat ground," *IEEE Transactions on Geoscience and Remote Sensing*, vol. 42, no. 2, pp. 318–326, 2004.

[12] A. Giannopoulos and N. Diamanti, "Numerical modelling of ground-penetrating radar response from rough subsurface interfaces," *Near Surface Geophysics*, vol. 6, no. 6, pp. 357–369, 2008.

[13] I. M. Fuks and A. G. Voronovich, "Wave diffraction by rough interfaces in an arbitrary plane-layered medium," *Waves in Random Media*, vol. 10, no. 2, pp. 253–72, 2000.

[14] A. Tabatabaeenejad and M. Moghaddam, "Bistatic scattering from three-dimensional layered rough surfaces," *IEEE Transactions on Geoscience and Remote Sensing*, vol. 44, no. 8, pp. 2102–14, 2006.

[15] M. A. Demir, J. T. Johnson, and T. J. Zajdel, "A study of the fourth-order small perturbation method for scattering from two-layer rough surfaces," *IEEE Transactions on Geoscience and Remote Sensing*, vol. 50, no. 9, pp. 3374–3382, 2012.

[16] S. Afifi and R. Dusséaux, "Scattering by anisotropic rough layered 2D interfaces," *IEEE Transactions on Antennas and Propagation*, vol. 60, no. 11, pp. 5315–5328, 2012.

[17] A. Soubret, G. Berginc, and C. Bourrely, "Application of reduced Rayleigh equations to electromagnetic wave scattering by two-dimensional randomly rough surfaces," *Physical Review B*, vol. 63, no. 24, p. 245411, 2001.

[18] I. M. Fuks, "Modeling of scattering by a rough surface of layered media," in *2002 IEEE International Geoscience and Remote Sensing Symposium*, vol. 2, Toronto, Ontario, Canada, 2002, pp. 1251–3.

[19] D. G. Blumberg, V. Freilikher, I. M. Fuks, Y. Kaganovskii, A. A. Maradudin, and M. Rosenbluh, "Effects of roughness on the retroreflection from dielectric layers," *Waves in Random Media*, vol. 12, no. 3, pp. 279–92, 2002.

[20] Z.-H. Gu, I. M. Fuks, and M. Ciftan, "Grazing angle enhanced backscattering from a dielectric film on a reflecting metal substrate," *Optical Engineering*, vol. 43, no. 3, pp. 559–67, 2004.

[21] N. Pinel, N. Déchamps, C. Bourlier, and J. Saillard, "Bistatic scattering from one-dimensional random rough homogeneous layers in the high-frequency limit with shadowing effect," *Waves in Random and Complex Media*, vol. 17, no. 3, pp. 283–303, 2007.

[22] N. Pinel, J. T. Johnson, and C. Bourlier, "A geometrical optics model of three dimensional scattering from a rough layer with two rough surfaces," *IEEE Transactions on Antennas and Propagation*, vol. 58, no. 3, pp. 809–816, 2010.

[23] N. Pinel, C. Bourlier, and J. Saillard, "Forward radar propagation over oil slicks on sea surfaces using the Ament model with shadowing effect," *Progress In Electromagnetics Research*, vol. 76, pp. 95–126, 2007.

[24] ——, "Degree of roughness of rough layers: extensions of the Rayleigh roughness criterion and some applications," *Progress In Electromagnetics Research B*, vol. 19, pp. 41–63, 2010.

[25] A. Tabatabaeenejad, X. Duan, and M. Moghaddam, "Coherent scattering of electromagnetic waves from two-layer rough surfaces within the Kirchhoff regime," *IEEE Transactions on Geoscience and Remote Sensing*, vol. 51, no. 7, pp. 3943–3953, 2013.

[26] E. Bahar and Y. Zhang, "Diffuse like and cross-polarized fields scattered from irregular layered structures-full-wave analysis," *IEEE Transactions on Antennas and Propagation*, vol. 47, no. 5, pp. 941–8, 1999.

[27] Y. Zhang and E. Bahar, "Mueller matrix elements that characterize scattering from coated random rough surfaces," *IEEE Transactions on Antennas and Propagation*, vol. 47, no. 5, pp. 949–55, 1999.

[28] G. Berginc and C. Bourrely, "The small-slope approximation method applied to a three-dimensional slab with rough boundaries," *Progress In Electromagnetics Research*, vol. 73, pp. 131–211, 2007.

[29] S. Tjuatja, A. K. Fung, and M. S. Dawson, "An analysis of scattering and emission from sea ice," *Remote Sensing Reviews*, vol. 7, pp. 83–106, 1993.

[30] P. Imperatore, A. Iodice, M. Pastorino, and N. Pinel, "Modelling scattering of electromagnetic waves in layered media: An up-to-date perspective," *International Journal of Antennas and Propagation*, p. 14, 2017.

[31] J. M. Elson, "Infrared light scattering from surfaces covered with multiple dielectric overlayers," *Applied Optics*, vol. 16, no. 11, pp. 2873–81, 1977.

[32] Z. Knittl, *Optics of thin films*. London: Wiley, 1976.

[33] J. M. Eastman, "Scattering by all-dielectric multilayer band-pass filters and mirrors for lasers," in *Physics of Thin Films*, G. Hass and M. H. Francombe, Eds. New York: Academic, 1978, vol. 10, pp. 167–226.

[34] I. Ohlídal and K. Navrátil, "Scattering of light from multilayer with rough boundaries," in *Progress in Optics*, E. Wolf, Ed. Elsevier Science, 1995, vol. XXXIV, pp. 248–331.

[35] C. Amra, "Light scattering from multilayer optics. I. Tools of investigation," *Journal of the Optical Society of America A*, vol. 11, no. 1, pp. 197–210, 1994.

[36] C.-H. Kuo and M. Moghaddam, "Scattering from multilayer rough surfaces based on the extended boundary condition method and truncated singular value decomposition," *IEEE Transactions on Antennas and Propagation*, vol. 54, no. 10, pp. 2917–29, 2006.

[37] P. Imperatore, A. Iodice, and D. Riccio, "Electromagnetic wave scattering from layered structures with an arbitrary number of rough interfaces," *IEEE Transactions on Geoscience and Remote Sensing*, vol. 47, no. 4, pp. 1056–72, 2009.

[38] S. Afifi, R. Dusséaux, and A. Berrouk, "Electromagnetic scattering from 3D layered structures with randomly rough interfaces: Analysis with the small perturbation method and the small slope approximation," *IEEE Transactions on Antennas and Propagation*, vol. 62, no. 10, pp. 5200–5208, 2014.

[39] H. Zamani, A. Tavakoli, and M. Dehmollaian, "Second-order perturbative solution of cross-polarized scattering from multilayered rough surfaces," *IEEE Transactions on Antennas and Propagation*, vol. 64, no. 5, pp. 1877–1890, 2016.

[40] T. Wang, L. Tsang, J. T. Johnson, and S. Tan, "Scattering and transmission of waves in multiple random rough surfaces: Energy conservation studies with the second order small perturbation method," *Progress In Electromagnetics Research*, vol. 157, pp. 1–20, 2016.

[41] F. Jonard, L. Weihermüller, H. Vereecken, and S. Lambot, "Accounting for soil surface roughness in the inversion of ultrawideband off-ground GPR signal for soil moisture retrieval," *Geophysics*, vol. 77, no. 1, pp. H1–H7, 2012.

[42] C. Warren, A. Giannopoulos, and I. Giannakis, "gprmax: Open source software to simulate electromagnetic wave propagation for ground penetrating radar," *Computer Physics Communications*, vol. 209, pp. 163–170, 2016.

[43] S. Lambot, E. C. Slob, I. van den Bosch, B. Stockbroeckx, and M. Vanclooster, "Modeling of ground-penetrating radar for accurate characterization of subsurface electric properties," *IEEE Transactions on Geoscience and Remote Sensing*, vol. 42, pp. 2555–2568, 2004.

[44] E. C. Slob and J. Fokkema, "Coupling effects of two electric dipoles on an interface," *Radio Science*, vol. 37, no. 5, pp. 1073, doi:1010.1029/2001RS002 529, 2002.

[45] S. Lambot, E. Slob, and H. Vereecken, "Fast evaluation of zero-offset Green's function for layered media with application to ground-penetrating radar," *Geophysical Research Letters*, vol. 34, pp. L21 405, doi:21 410.21 029/22 007GL031 459, 2007.

[46] A. K. Fung, Z. Li, and K. S. Chen, "Backscattering from a randomly rough dielectric surface," *IEEE Transactions on Geoscience and Remote Sensing*, vol. 30, no. 2, pp. 356–369, 1992.
[47] W. S. Ament, "Toward a theory of reflection by a rough surface," *Proceedings of the Institute of Radio Engineers*, vol. 41, no. 1, pp. 142–146, 1953.
[48] P. Beckmann and A. Spizzichino, *The scattering of electromagnetic waves from rough surfaces*. 2nd ed., Berlin, Germany: Springer Verlag, 1987.
[49] D. Freund, N. Woods, H. Ku, and R. Awadallah, "The effects of shadowing on modelling forward radar propagation over a rough sea surface," *Waves in Random and Complex Media*, vol. 18, no. 3, pp. 387–408, 2008.
[50] O. Landron, M. J. Feuerstein, and T. S. Rappaport, "A comparison of theoretical and empirical reflection coefficients for typical exterior wall surfaces in a mobile radio environment," *IEEE Transactions on Antennas and Propagation*, vol. 44, no. 3, pp. 341–351, 1996.
[51] K. S. Yee, "Numerical solution of initial boundary value problems involving maxwell's equations in isotropic media," *Antennas and Propagation, IEEE Transactions on*, vol. 14, no. 3, pp. 302–307, 1966.
[52] A. Giannopoulos, "Unsplit implementation of higher order pmls," *IEEE Transactions on Antennas and Propagation*, vol. 60, no. 3, pp. 1479–1485.
[53] D. Correia and J. Jin, "On the development of a higher-order pml," *IEEE Transactions on Antennas and Propagation*, vol. 53, no. 12, pp. 4157–4163, 2005.
[54] S. D. Gedney and B. Zhao, "An auxiliary differential equation formulation for the complex-frequency shifted pml," *IEEE Transactions on Antennas and Propagation*, vol. 58, no. 3, pp. 838–847, 2010.
[55] N. Feng and J. Li, "Novel and efficient fdtd implementation of higher-order perfectly matched layer based on ade method," *Journal OF Computational Physics*, vol. 232, no. 1, pp. 318–326, 2013.
[56] N. Feng, J. Li, and X. Zhao, "Efficient fdtd implementations of the higher-order pml using dsp techniques for arbitrary media," *IEEE Transactions on Antennas and Propagation*, vol. 61, no. 5, pp. 2623–2629, 2013.
[57] A. Giannopoulos, "Multipole perfectly matched layer for finite-difference time-domain electromagnetic modeling," *IEEE Transactions on Antennas and Propagation*, vol. 66, no. 6, pp. 2987–2995, 2018.
[58] S. Lambot and F. André, "Full-wave modeling of near-field radar data for planar layered media reconstruction," *IEEE Transactions on Geoscience and Remote Sensing*, vol. 52, no. 5, pp. 2295 – 2303, 2014.
[59] W. Huyer and A. Neumaier, "Global optimization by multilevel coordinate search," *Journal of Global Optimization*, vol. 14, no. 4, pp. 331–355, 1999.

FIGURES

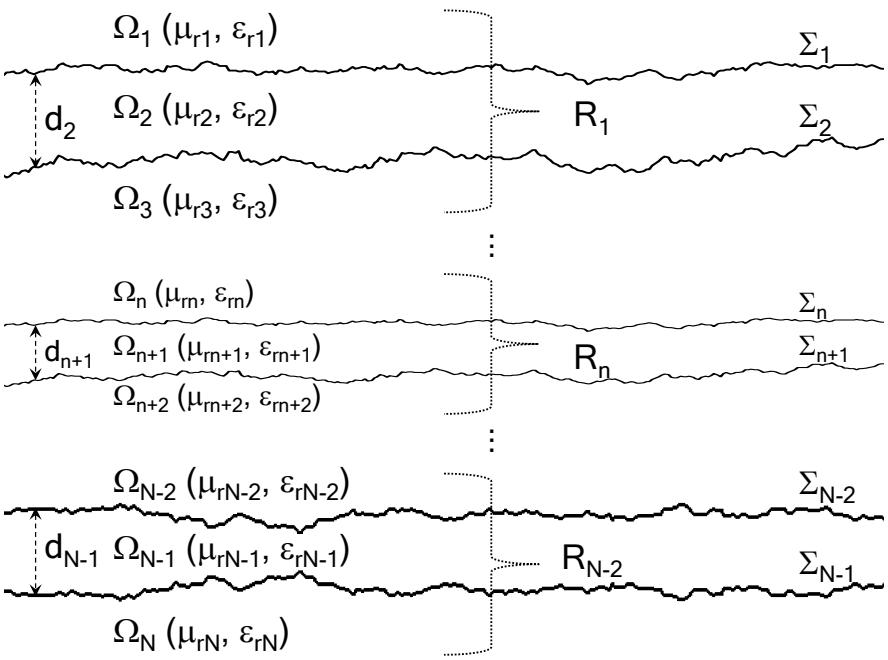

Fig. 1. Three-dimensional planar multilayered medium with rough interfaces (Σ_n is the interface n, Ω_n is the layer n characterized by a dielectric permittivity ϵ_n, a magnetic permeability μ_n, and a thickness d_n, and R_n is the equivalent Fresnel reflection coefficient).

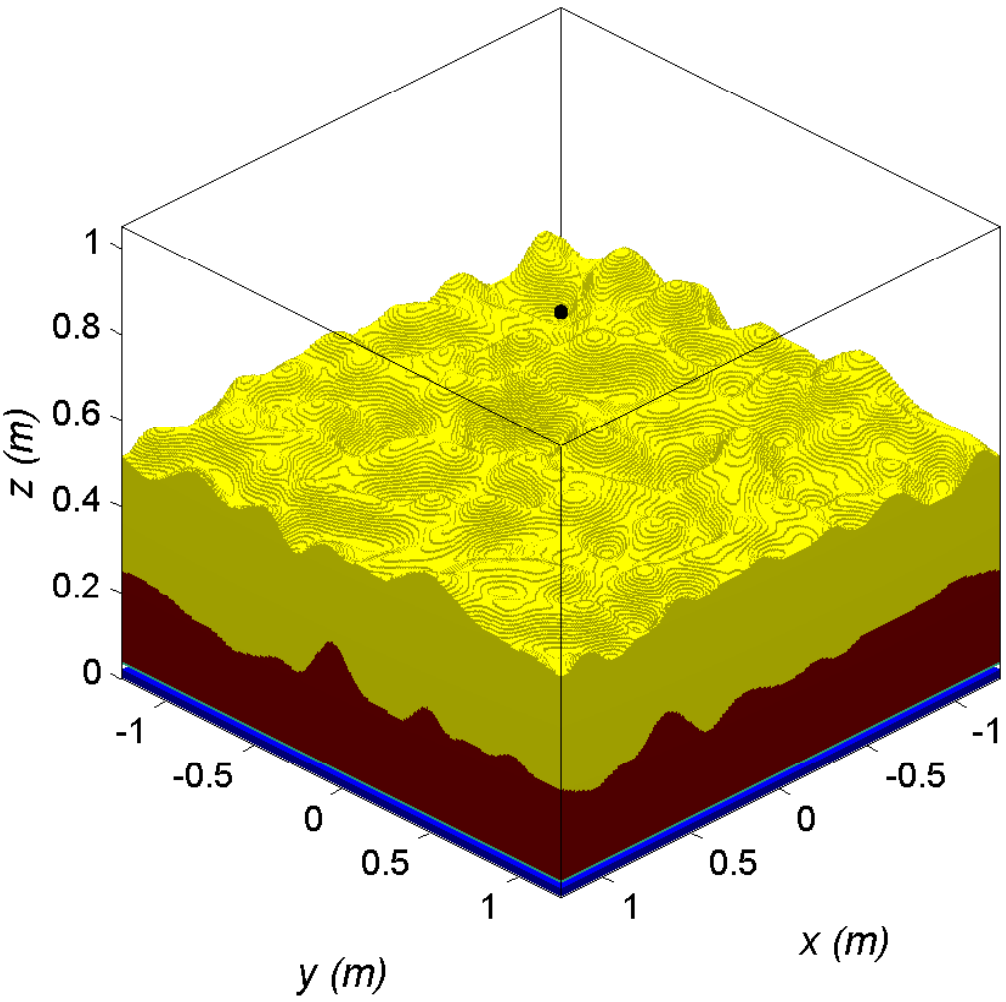

Fig. 2. Geometrical model used for the FDTD simulations with a spatial domain of $2.5 \times 2.5 \times 1.05$ m, and a spatial resolution of 0.0025 m. The position of the source and receiver is at $z = 0.85$ m, and in the centre of the $x - y$ plane.

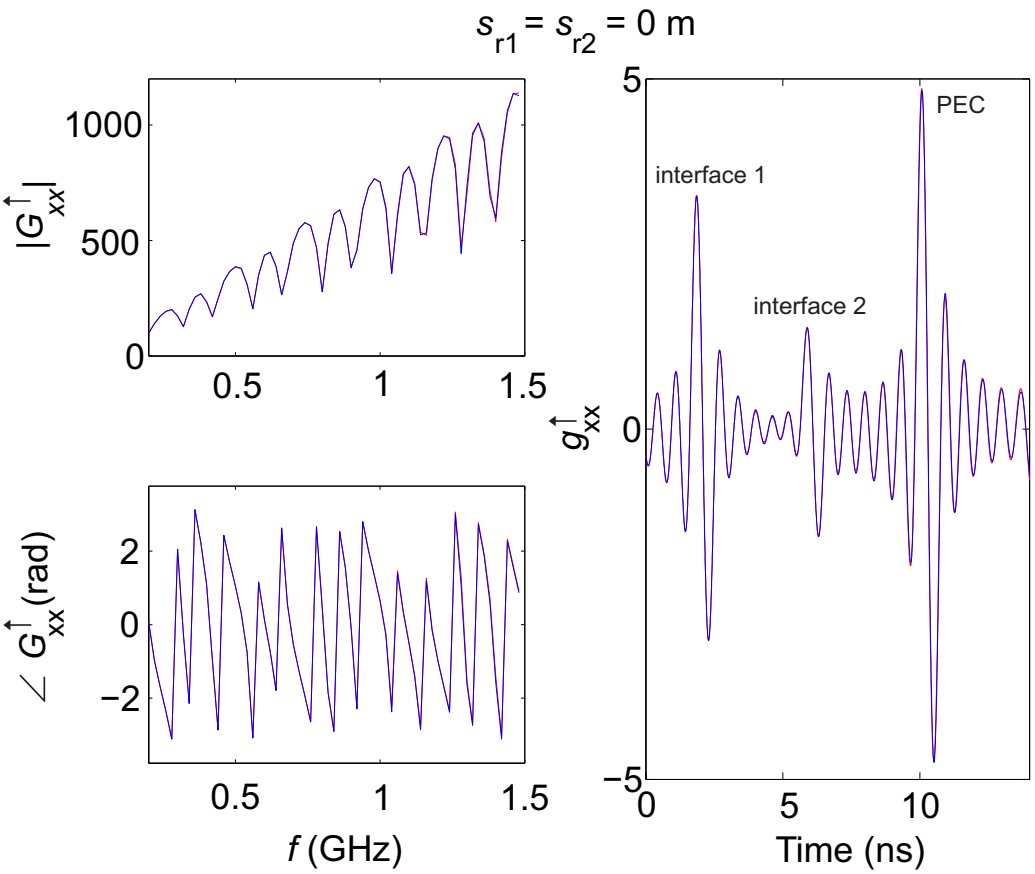

Fig. 3. Green's functions computed by our asymptotic extended SKA model (red curves) and the FDTD simulations (blue curves) in the frequency (frequency range 0.2–1.5 GHz) and time (time window 0–14 ns) domains for perfectly flat interfaces ($s_{r1} = s_{r2} = 0$).

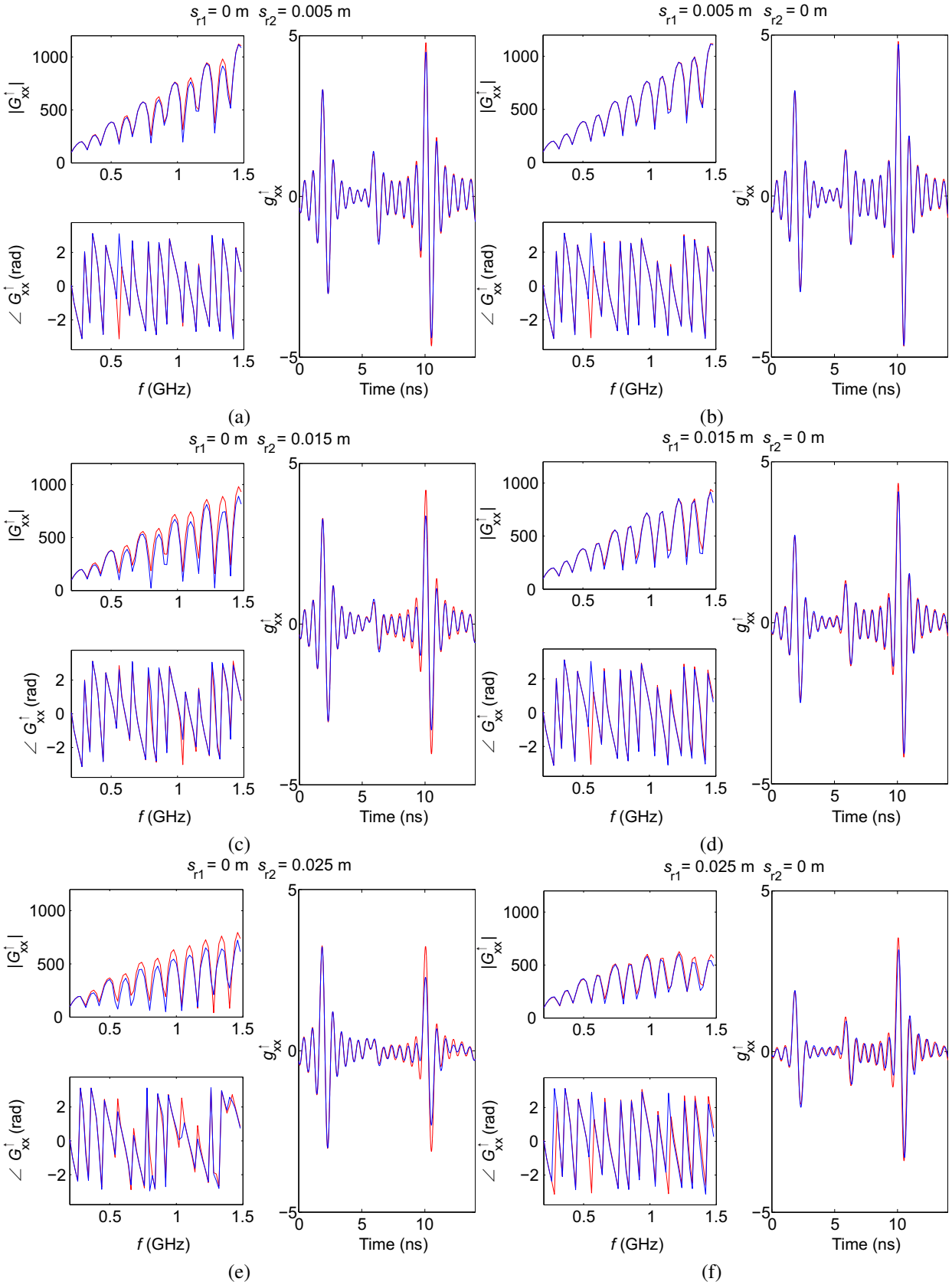

Fig. 4. Green's functions computed by our asymptotic extended SKA model (red curves) and the FDTD simulations (blue curves) in the frequency and time domains, for rough interfaces with different RMS values of the surface heights (s_{r1} and s_{r2}). Smooth top interface $s_{r1} = 0$ (left) and smooth intermediate interface (right) $s_{r2} = 0$. The relative dielectric permittivity of the top layer is 4, while the relative permittivity of the bottom layer is 10. The top layer has an average thickness of 30 cm, while the bottom layer has an average thickness of 20 cm.

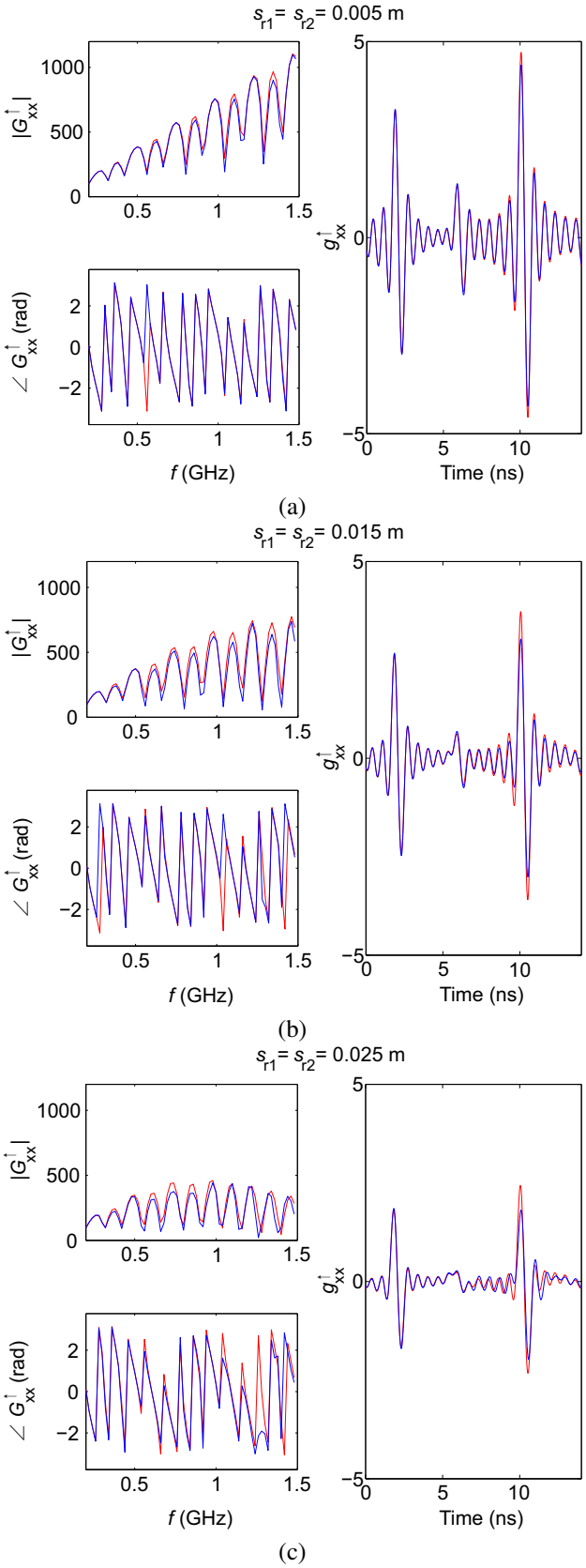

Fig. 5. Green's functions computed by our asymptotic extended SKA model (red curves) and the FDTD simulations (blue curves) in the frequency and time domains, for rough interfaces with RMS values of the surface heights (s_{r1} and s_{r2}) between 0.005 and 0.025 m. The relative dielectric permittivity of the top layer is 4, while the relative permittivity of the bottom layer is 10. The top layer has an average thickness of 30 cm, while the bottom layer has an average thickness of 20 cm.

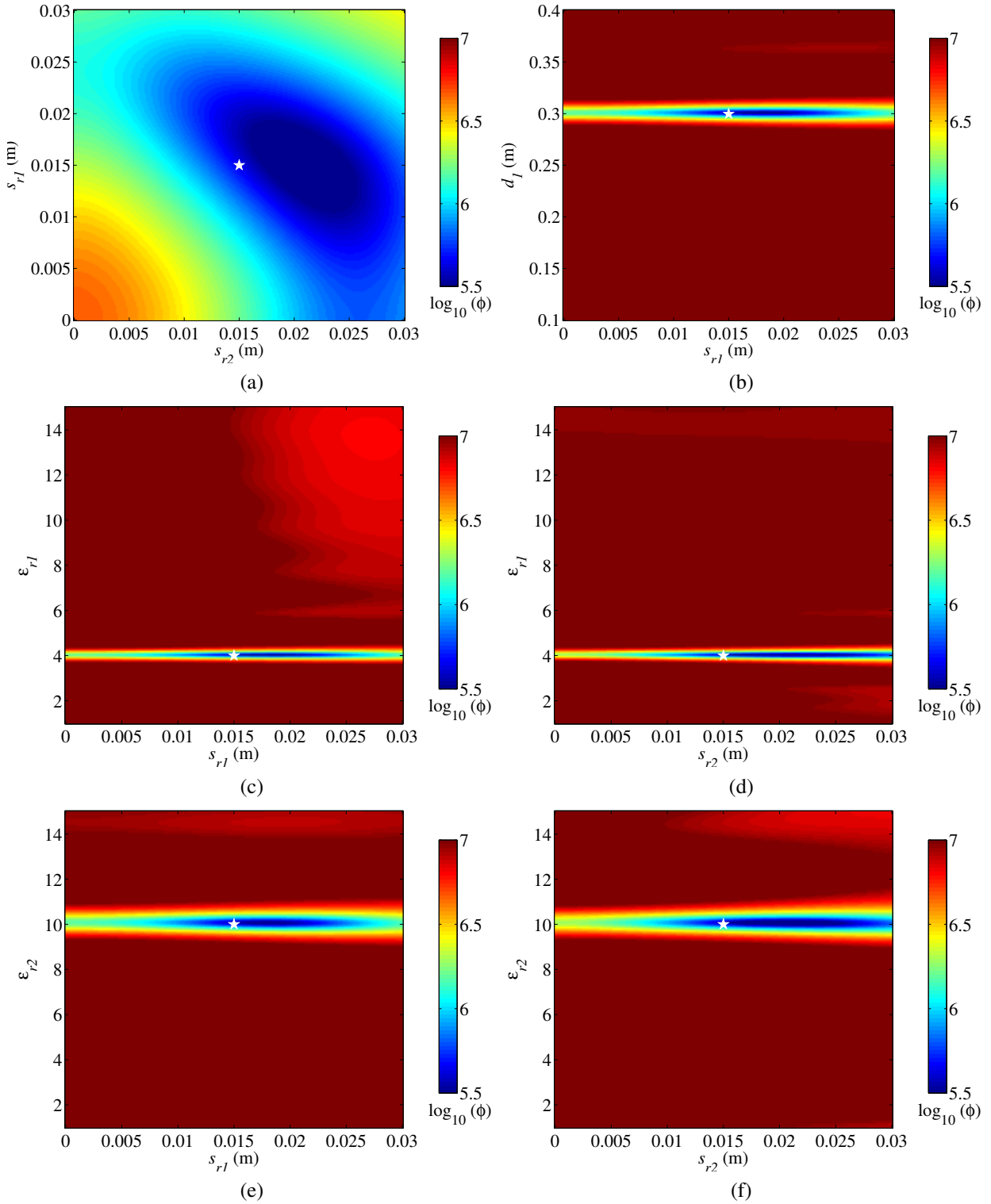

Fig. 6. Sections of the objective function logarithm $\log_{10}(\phi(\mathbf{p}))$ for inversion of the roughness model in the $s_{r1} - s_{r2}$ (a), $d_1 - s_{r1}$ (b), $\epsilon_{r1} - s_{r1}$ (c), $\epsilon_{r1} - s_{r2}$ (d), $\epsilon_{r2} - s_{r1}$ (e), and $\epsilon_{r2} - s_{r2}$ (f) parameter planes. The asterisk represents the true parameter values.

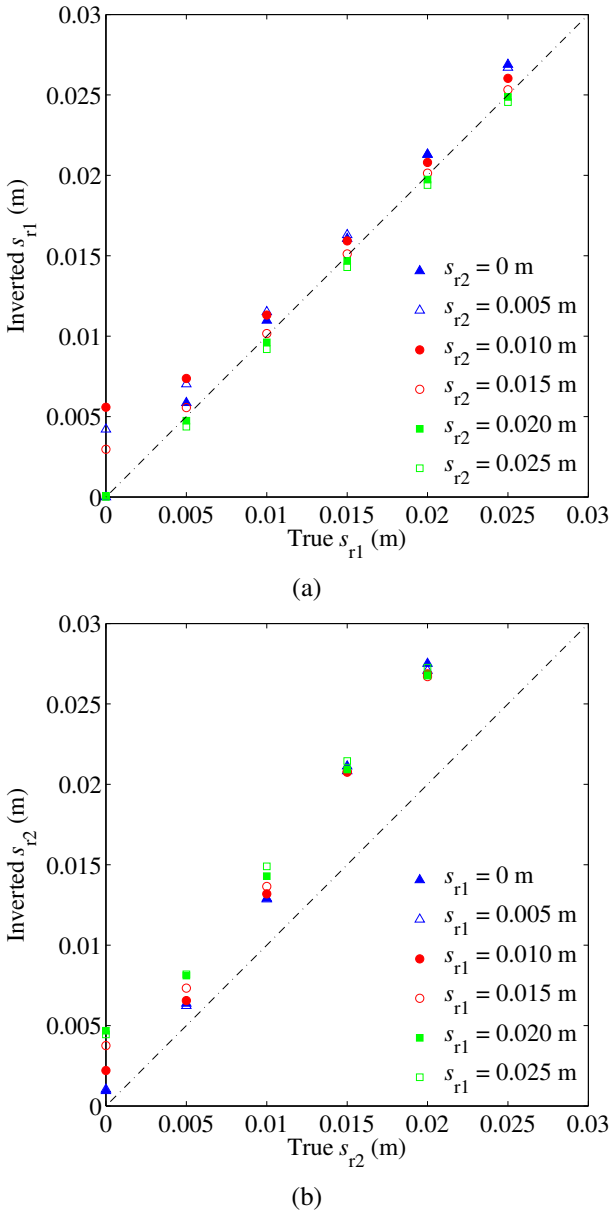

Fig. 7. Comparison of the true (i.e., s_r values used to generate the 50 Monte-Carlo FDTD simulations) and inversely estimated RMS of the surface heights: (a) of the first interface, and (b) of the second interface.